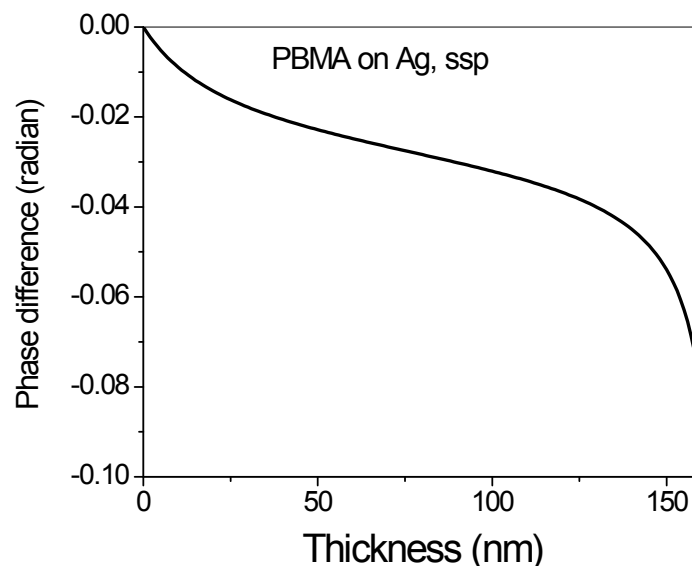


## Illustrating consistency of different experimental approaches to probe the buried polymer/metal interface using sum frequency generation vibrational spectroscopy

*Xiaolin Lu, Bolin Li, Peizhi Zhu, Gi Xue, Dawei Li*

### Reconstruction of the ssp spectra for the PBMA films on the Ag substrates

To reconstruct the ssp spectra of the PBMA films on the Ag substrates, we need to know the normalized resonant modes of the PBMA surface in air and the PBMA/Ag interface. From the fitting results in Table 1 for the PBMA ssp surface spectrum, we know all the resonant modes at the surface. Since the Fresnel coefficient for the ssp polarization combination is 0.20, the normalized strengths of all the resonant modes for the PBMA surface in air can be obtained. For example, in Table 1, the strength ( $A_q$ ) of the ss mode is 7.5; after divided by 0.20, the normalized strength of the ss mode is 38.



**Figure S1.** Phase difference ( $\alpha$ ) between the output resonant signals from the PBMA surface in air and the PBMA/Ag interface.

For the PBMA/Ag interface, there are four measurements for the sandwiched PBMA thin films corresponding to the four different thicknesses (24 nm, 56 nm, 85 nm, and 113 nm). The averaged strengths are used. The Fresnel coefficient for the ssp polarization combination is almost a constant ( $\sim 0.33$ ) no matter what the film thickness is (Figure 4 in the main text).

The following equation is used to reconstruct the spectra.

$$I_{ssp} \propto |\chi_{eff,ssp}|^2 = \left| \chi_{NR} e^{i\beta} + F_{PBMA/Air,ssp} \sum_q \frac{A_q e^{i\alpha}}{\omega - \omega_q + i\Gamma_q} + F_{PBMA/Ag,ssp} \sum_q \frac{A_q}{\omega - \omega_q + i\Gamma_q} \right|^2$$

There are three terms in this equation. The first term accounts for the non-resonant

background and its relative phase to the molecular resonant terms. The second term is responsible for the resonant contribution from the PBMA surface in air and  $F_{PBMA/Air,ssp}$  can be read from Panel A of Figure 6. The third term is responsible for the resonant contribution from the PBMA/Ag interface and  $F_{PBMA/Ag,ssp}$  can be read from Panel A of Figure 6 in the main text. In the second term there is a term  $e^{i\alpha}$ , which is responsible for the propagation phase difference between the surface and interfacial resonant contributions since finally they must coherently add up together [S1, S2]. We calculate the phase term of  $\alpha$  as a function of the film thickness and put it the Figure S1. Now, in order to reconstruct the spectra, only  $\chi_{NR}$  and  $\beta$  need to be adjusted. Table S1 list the  $\chi_{NR}$  and  $\beta$  used to reconstruct the spectra in Panel B of Figure 5 in the main text.

**Table S1.** The listed  $\chi_{NR}$  and  $\beta$  as two parameters to reconstruct the ssp spectra of the PBMA thin films on the Ag substrates.

Thickness (nm)	$\chi_{NR}$	$\beta$
11	6.0	1.0
33	11.6	0.7
45	14.6	0.9
127	10.0	0.9

### Calculation of the tilt angle of the ester butyl methyl groups

From the measurement of different polarization combinations, the following effective nonlinear susceptibility components can be detected [S3].

$$\begin{aligned}\chi_{eff,ssp}^{(2)} &= L_{yy}(\omega)L_{yy}(\omega_1)L_{zz}(\omega_2)\sin\varphi_2\chi_{yyz} = F_{ssp,yyz}\chi_{yyz} \\ \chi_{eff,ppp}^{(2)} &= -L_{xx}(\omega)L_{xx}(\omega_1)L_{zz}(\omega_2)\cos\varphi\cos\varphi_1\sin\varphi_2\chi_{xxz} + L_{xx}(\omega)L_{zz}(\omega_1)L_{xx}(\omega_2)\cos\varphi\sin\varphi_1\cos\varphi_2\chi_{xxz} \\ &\quad + L_{zz}(\omega)L_{xx}(\omega_1)L_{xx}(\omega_2)\sin\varphi\cos\varphi_1\cos\varphi_2\chi_{xxx} + L_{zz}(\omega)L_{zz}(\omega_1)L_{zz}(\omega_2)\sin\varphi\sin\varphi_1\sin\varphi_2\chi_{zzz} \\ &\cong -L_{xx}(\omega)L_{xx}(\omega_1)L_{zz}(\omega_2)\cos\varphi\cos\varphi_1\sin\varphi_2\chi_{xxz} + L_{zz}(\omega)L_{zz}(\omega_1)L_{zz}(\omega_2)\sin\varphi\sin\varphi_1\sin\varphi_2\chi_{zzz} \\ &= F_{ppp,xxz}\chi_{xxz} + F_{ppp,zzz}\chi_{zzz}\end{aligned}$$

For an azimuthally isotropic surface or interface, there are only four independent components for the second nonlinear susceptibility tensor components [S4].

$$\chi_{xxz} = \chi_{yyz}, \chi_{xxz} = \chi_{zyy}, \chi_{xxx} = \chi_{zyy}, \chi_{zzz}$$

For the ester butyl methyl groups, a  $C_{3v}$  symmetry is assumed. The second-order nonlinear susceptibility in the lab coordinate system and the molecular hyperpolarizability in the molecular coordinate system can be related through the following functions [S5, S6].

For the symmetric stretching (ss) mode,

$$\chi_{yyz,ss} = \chi_{xxz,ss} = \frac{1}{2}N_s\beta_{ccc,ss}\left[\cos\theta(1+r) - \cos^3\theta(1-r)\right]$$

$$\chi_{xx,ss} = \chi_{yy,ss} = \chi_{zz,ss} = \chi_{xy,ss} = \frac{1}{2} N_s \beta_{ccc,ss} (\cos \theta - \cos^3 \theta) (1-r)$$

$$\chi_{zz,ss} = N_s \beta_{ccc,ss} [r \cos \theta + \cos^3 \theta (1-r)]$$

$$\text{Here } r = \beta_{aac,ss} / \beta_{ccc,ss}$$

For the antisymmetric stretching (as) mode,

$$\chi_{yz,as} = \chi_{xz,as} = -N_s \beta_{caa,as} (\cos \theta - \cos^3 \theta)$$

$$\chi_{xx,as} = \chi_{yy,as} = \chi_{zz,as} = \chi_{xy,as} = N_s \beta_{caa,as} \cos^3 \theta$$

$$\chi_{zz,as} = 2N_s \beta_{caa,as} (\cos \theta - \cos^3 \theta)$$

As we know, at a surface or interface, a large number of molecules or molecular groups may not adopt the same tilt angle and a distribution function could be a better representation for the real case. The Gaussian function has been used to represent the real angle distribution [S7, S8].

$$f(\theta) = C \exp\left[-\frac{(\theta - \theta_0)^2}{2\sigma^2}\right]$$

For a trigonometric function of “ $\cos \theta$ ”, after applying the Gaussian distribution, it becomes

$$\langle \cos \theta \rangle = \int \cos \theta f(\theta) \sin \theta d\theta$$

Here  $\sigma$  is the root-mean-square width and C is a normalization constant.

Previous study suggested the uncertainty of the r value, which is between 1.6 and 4.2 [S5]. Here the middle value of  $r=3.0$  is used to deduce the possible tilt angle of the ester butyl methyl groups. From the calculation of the Fresnel coefficients, we find

$$F_{ssp,yyz} = 0.20, F_{ppp,xxz} = -0.16, F_{ppp,zzz} = 0.19$$

So we obtain the following equation related to the tilt angle of ester butyl methyl groups at the PBMA surface in air.

$$\left| \frac{\chi_{eff,ssp,ss}^{(2)}}{\chi_{eff,ppp,as}^{(2)}} \right| \cong \left| \frac{F_{ssp,yyz} \chi_{yyz,ss}}{F_{ppp,xxz} \chi_{xxz,as} + F_{ppp,zzz} \chi_{zzz,as}} \right| = \left| \frac{0.40 \cos \theta + 0.20 \cos^3 \theta}{1.51 (\cos \theta - \cos^3 \theta)} \right|$$

Using the similar method but for the sandwiched geometry, we obtain the equation related to the tilt angle of ester butyl methyl groups at the PBMA/Ag interface.

$$\left| \frac{\chi_{eff,ssp,as}^{(2)}}{\chi_{eff,ppp,ss}^{(2)}} \right| \cong \left| \frac{F_{ssp,yyz} \chi_{yyz,as}}{F_{ppp,xxz} \chi_{xxz,as} + F_{ppp,zzz} \chi_{zzz,as}} \right| = \left| \frac{0.90 (\cos \theta - \cos^3 \theta)}{3.1 \cos \theta - 0.79 \cos^3 \theta} \right|$$

The experimental value was obtained based on the fitting results. For the PBMA surface in air, using the intensity ratio of ss mode in ssp spectrum and as mode in ppp spectra (Figure 2 and Table 1 in the main text), we can obtain

$$\left| \frac{\chi_{eff,ssp,ss}^{(2)}}{\chi_{eff,ppp,as}^{(2)}} \right|_{Experimental} = \left| \frac{A_{ssp,2880}/\Gamma_{ssp,2880} + A_{ssp,2935}/\Gamma_{ssp,2935}}{A_{ppp,2960}/\Gamma_{ppp,2960}} \right| = 2.4$$

Similarly, for the PBMA/Ag interface, we can find the experimental value

$$\left| \frac{\chi_{eff,ssp,as}^{(2)}}{\chi_{eff,ppp,ss}^{(2)}} \right|_{Experimental} = \left| \frac{A_{ssp,2956}/\Gamma_{ssp,2956}}{A_{ppp,2875}/\Gamma_{ppp,2875} + A_{ppp,2935}/\Gamma_{ppp,2935}} \right| = 0.28$$

### Refractive indexes used in this study.

Medium	Refractive index at sum frequency	Refractive index at visible frequency	Refractive index at infrared frequency
Air	1	1	1
Silica	1.46	1.46	1.41
PBMA	1.48	1.48	1.50
Ag	1.05+25.02i	0.056+3.06i	0.045+2.76i
PBMA/Air	1.20	1.20	1.20
Silica/PBMA	1.47	1.47	1.46
PBMA/Ag	1.48	1.48	1.50

Footnote: We chose the refractive indexes of the PBMA surface in air (PBMA/Air) as 1.20 referring to a previous slab model [S3]. The refractive indexes of the silica/PBMA were chosen as the intermediate between the adjacent two bulk media [S9, S10]. For the PBMA/Ag interface, the resonant signals were generated from the PBMA layer at the PBMA/Ag interface, such a PBMA layer belongs to the PBMA side. As treated by our previous studies [S11, S12], the bulk PBMA refractive indexes were used for the PBMA/Ag interface.

### References:

- S1. S. J. McCall, P. B. Davies, D. J. Neivandt *J. Phys. Chem. B* **2004**, 108, 16030-16039.
- S2. Y. Tong, Y. Zhao, N. Li, M. Osawa, P. B. Davies, S. Ye *J. Chem. Phys.* **2010**, 133, 034704.
- S3. X. Zhuang, P. B. Miranda, D. Kim, Y. R. Shen *Phys. Rev. B* **1999**, 59, 12632-12640.
- S4. P. Guyot-Sionnest, J. H. Hunt, Y. R. Shen *Phys. Rev. Lett.* **1987**, 59, 1597-1600.
- S5. C. Hirose, N. Akamatsu, K. Domen *Appl. Spectrosc.* **1992**, 46, 1051-1072.
- S6. C. Hirose, N. Akamatsu, K. Domen *J. Chem. Phys.* **1992**, 96, 997-1004.
- S7. X. Wei, X. Zhuang, S. C. Hong, T. Goto, Y. R. Shen *Phys. Rev. Lett.* **1999**, 82, 4256-4259.
- S8. G. J. Simpson, L. K. Rowlen *J. Am. Chem. Soc.* **1999**, 121, 2635-2636.

- S9. G. J. Simpson, S. Westerbuhr, K. L. Rowlen *Anal. Chem.* **2000**, 72, 887-898.
- S10. J. A. Ekhoﬀ, K. L. Rowlen *Anal. Chem.* **2002**, 74, 5954-5959.
- S11. X. Lu, G. Xue, X. Wang, J. Han, X. Han, J. Hankett, D. Li, Z. Chen  
*Macromolecules* **2012**, 45, 6087-6094.
- S12. Y. Fang, B. Li, J. Yu, J. Zhou, X. Xu, W. Shao, X. Lu *Surf. Sci.* **2013**, 615, 26-32.